ChemComm

RSC Publishing

COMMUNICATION

View Article Online
View Journal | View Issue



# Control of aggregation-induced emission by DNA hybridization†

Cite this: *Chem. Commun.*, 2013, **49**, 5835

Received 12th April 2013,
Accepted 9th May 2013

DOI: 10.1039/c3cc42706d

www.rsc.org/chemcomm

Shaoguang Li, Simon M. Langenegger and Robert Häner*

**Aggregation-induced emission (AIE) was studied by hybridization of dialkynyl-tetraphenylethylene (DATPE) modified DNA strands. Molecular aggregation and fluorescence of DATPEs are controlled by duplex formation.**

DNA is a useful and versatile scaffold for the assembly of functional groups with important applications in the fields of diagnostics, electronics, and materials science.[1–13] In particular, the introduction of a wide range of chromophores into DNA has drawn considerable attention.[14–23] Distinct photophysical effects are observed in such DNA-organized architectures including the formation of exciplexes,[24–28] H- and/or J-aggregates[29–31] or distinct helical arrangements with unique optical or chiral properties.[32–39] In recent years, tetraphenylethylene (TPE) and related molecules have attracted interest because of their unusual fluorescence properties. These chromophores are weakly or non-emissive as unassociated monomers but they become strongly fluorescent upon aggregation. Aggregation-induced emission (AIE) is a result of restricted intramolecular rotation in the aggregated state (Fig. 1a).[40,41] AIE features are of interest in diverse areas including fluorescence sensors[42] and OLEDs.[40] However, reports describing the interaction of AIE molecules (AIEs) with DNA,[43] proteins[44,45] or other bio-structures[46] are limited and only one recent publication has reported the incorporation of an AIE-active silole derivative into DNA strands using an enzymatic method.[47] Herein, we describe the synthesis and incorporation of the two stereoisomers of a dialkynyl-tetraphenylethylene (DATPE) into DNA and the AIE properties of the obtained conjugates (Fig. 1b).

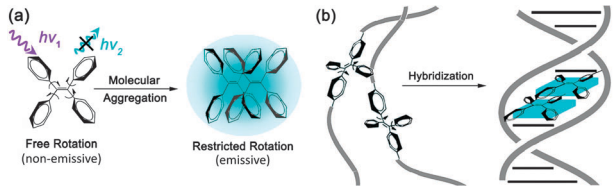


**Fig. 1** AIE properties of tetraphenylethylene (a) as a monomer and (b) as a building block in single and double stranded DNA.

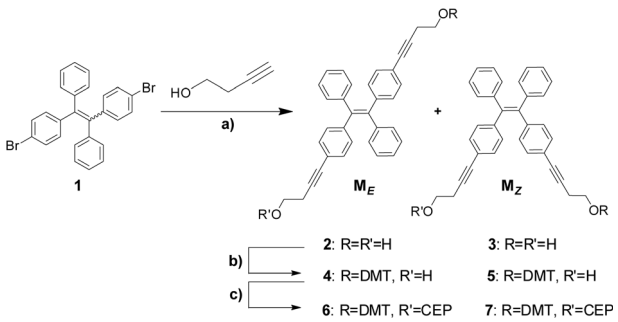


**Scheme 1** Preparation of phosphoramidites **6** and **7**; (a) CuI, $Pd(PPh_3)_2Cl_2$, $NEt_3$, THF; 38%; (b) DMTCl, THF, pyridine; 29% for **4**; 23% for **5**; (c) CEPCl, Hünig's base, DCM; DMT = 4,4′-dimethoxytrityl; CEP = 2-cyanoethyl-*N*,*N*-diisopropyl-phosphoramidite; 61% for **6**; 71% for **7**.

The synthetic strategy of the two building blocks ($\mathbf{M}_E$ and $\mathbf{M}_Z$) is shown in Scheme 1. Compound **1** was obtained according to the reported procedure as a mixture of *E*-/*Z*-isomers.[43] The butynyl chains were introduced through Sonogashira coupling using 3-butyn-1-ol. The *E*- and *Z*-isomers (**2** and **3**) were separated by chromatography and obtained in nearly equal amounts. The products were recrystallized and their configurations established by X-ray crystallography (ESI†). Compounds **2** and **3** exhibited typical AIE characteristics. They are non-emissive in well-solubilizing solvents, such as THF. In THF–water mixtures, the fluorescence intensity strongly increases once the water fraction rises above 60%. In a 95/5 (v/v) water–THF solution the quantum yields ($\Phi_F$, ESI†) are 0.40 and 0.39 for **2** and **3**, which compare well with similar compounds.[40]

The two diols were transformed into the corresponding mono-DMT protected alcohols **4** and **5**, which were subsequently converted into phosphoramidites **6** and **7**. These building blocks were used in the automated synthesis of oligomers **ON1-8** (Table 1) containing one or two DATPEs. All oligomers were purified by reversed-phase HPLC and characterized by ESI-MS (see ESI†).

*Department of Chemistry and Biochemistry, University of Bern, Freiestrasse 3, CH-3012 Bern, Switzerland. E-mail: robert.haener@ioc.unibe.ch; Tel: +41 31 631 4382*

† Electronic supplementary information (ESI) available: Synthetic and analytical details; additional spectroscopic data; X-ray structures. See DOI: 10.1039/c3cc42706d

**Table 1** Oligonucleotides (ONs) containing *E*- or *Z*-DATPE building blocks ($\mathbf{M}_E$ and $\mathbf{M}_Z$) and $T_m$ values of DNA hybrids

| | | Sequence | $T_m$[a] (°C) | $\Delta T_m$[b] (°C) |
|---|---|---|---|---|
| $\mathbf{D_R}$ | **R1** | 5′-AGC TCG GTC ATC GAG AGT GCA | 45.0 | — |
| | **R2** | 3′-TCG AGC CAG TAG CTC TCA CGT | | |
| **D1** | **ON1** | 5′-AGC TCG GTC A$\mathbf{M}_E$C GAG AGT GCA | 47.0 | 2.0 |
| | **ON2** | 3′-TCG AGC CAG T$\mathbf{M}_E$G CTC TCA CGT | | |
| **D2** | **ON3** | 5′-AGC TCG GTC A$\mathbf{M}_Z$C GAG AGT GCA | 47.0 | 2.0 |
| | **ON4** | 3′-TCG AGC CAG T$\mathbf{M}_Z$G CTC TCA CGT | | |
| **D3** | **ON5** | 5′-AGC TCG GTC $\mathbf{M}_E\mathbf{M}_E$C GAG AGT GCA | 49.5 | 4.5 |
| | **ON6** | 3′-TCG AGC CAG $\mathbf{M}_E\mathbf{M}_E$G CTC TCA CGT | | |
| **D4** | **ON7** | 5′-AGC TCG GTC $\mathbf{M}_Z\mathbf{M}_Z$C GAG AGT GCA | 50.0 | 5.0 |
| | **ON8** | 3′-TCG AGC CAG $\mathbf{M}_Z\mathbf{M}_Z$G CTC TCA CGT | | |

[a] Conditions: 1.0 μM oligonucleotide (each strand), 10 mM sodium phosphate buffer (pH 7.4) and 100 mM NaCl, recorded in 2,2,2-trifluorethanol–water (70/30 v/v). [b] Compared to unmodified duplex $\mathbf{D_R}$.

A mixed solvent system composed of a buffered system with 2,2,2-trifluoroethanol (TFE, 70%, v/v) and water (30%, v/v, ESI†)[48] was used to analyze the spectroscopic properties of the DATPE-modified oligonucleotides.[49] Measurements performed in buffered water alone or smaller fractions of TFE provided qualitatively similar results but the effects were less pronounced. Generally, single strands showed considerably weaker fluorescence in TFE–water mixtures than in water alone. We ascribe this to reduced molecular interactions between DATPE and the nucleotides and, consequently, to increased internal rotation in DATPEs[42] in the presence of the less polar TFE.

The melting temperature ($T_m$) values of the different hybrids obtained by thermal denaturation are summarized in Table 1. The DATPE units have a positive effect on the stability of the duplex with $\Delta T_m$ values ranging from +2 to +5 °C, for hybrids containing two or four DATPE units, respectively. This stabilization can be attributed to favorable stacking interactions between the propeller-twisted DATPE molecules in the duplex.

The UV-vis and fluorescence spectra recorded for hybrid **D1** are shown in Fig. 2 along with the spectra of the single strands. For the single strand **ON1**, the absorption band of the *E*-DATPE molecule locates around 327 nm. The maximum of this band is shifted to 335 nm during formation of the duplex **D1**. Aggregation of the two DATPE molecules by hybridization of the two single strands results in a considerable enhancement of the fluorescence intensity (Fig. 2, right). The fluorescence intensity of **D1** at 490 nm is about 9 times higher than that of **ON1** and roughly 3 times higher than that of **ON2**. These differences were also reflected in the fluorescence quantum yields ($\Phi_F$) given in Table 2. $\Phi_F$ rises to 0.22 upon hybridization compared to 0.05 and 0.10 for **ON1** and **ON2**, respectively. Similar effects are observed for **D2** containing two *Z*-isomers. Fig. 3 displays the titration of **ON3** with **ON4**, in which $\Phi_F$ gradually increases to 0.19 in the duplex **D2**.

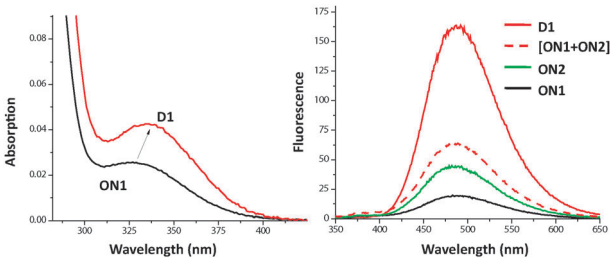


**Fig. 2** Left: absorption spectra of single strands **ON1** and **D1**; right: fluorescence spectra of **ON1**, **ON2**, calculated sum of spectra of **ON1** and **ON2**, and **D1** (20 °C; $\lambda_{ex}$: 335 nm, ex. slit: 5 nm; em. slit: 5 nm; detector: 600 V; other conditions as in Table 1; for more details see ESI†).

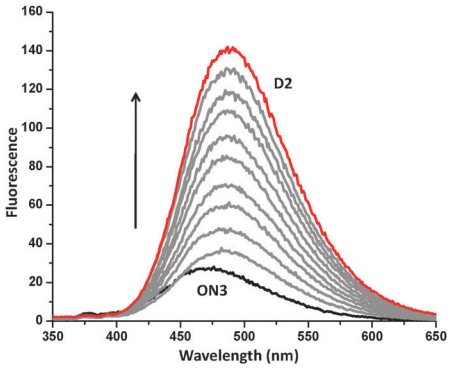


**Fig. 3** Change of fluorescence by addition of **ON4** (individual steps = 0.1 μM; conditions as in Fig 2) to **ON3**; arrow: increasing **ON4** conc.

Formation of the duplex results in a gradual shift in the emission maximum from 476 nm (**ON3**) to 490 nm for **D2**. Fluorescence intensity is significantly increased by annealing of the two strands (an increase by a factor of 5.6 compared to **ON3**, Fig. 3), indicating a restriction of internal rotation by aggregation of the two DATPEs.[41,42] Thus, the AIE character of the building blocks is controlled by the hybridization process. Emission maxima and quantum yields are summarized in Table 2.

Fig. 4 illustrates the effect of molecular aggregation of DATPEs by DNA hybridization. The comparison between **ON7** and **D2** shows that the emission by two DATPE molecules is considerably higher in the duplex ($\Phi_F$ = 0.19) than in the single strand ($\Phi_F$ = 0.07). This is expected since the molecular aggregation should be positively influenced by the well-organized duplex structure compared to the single stranded random coil. A further extension of the DATPE stack, as in **D4**, results in a further significant increase in the fluorescence intensity ($\Phi_F$ = 0.32). The $\Phi_F$ values of **D3** and **D4** are three times higher than those of the corresponding single strands and close to the monomeric building blocks **2** and **3** in their aggregated states

**Table 2** Emission maxima and quantum yields ($\Phi_F$) of *E*- and *Z*-DATPE molecules (**2** and **3**) and modified single strands and hybrids (quinine sulfate as standard, for conditions see Table 1 and ESI)

| | ***E*-DATPE (2)**[a] | ***Z*-DATPE (3)**[a] | **ON1** | **ON2** | **D1** | **ON3** | **ON4** | **D2** | **ON5** | **ON6** | **D3** | **ON7** | **ON8** | **D4** |
|---|---|---|---|---|---|---|---|---|---|---|---|---|---|---|
| $\lambda_{max}$ (nm) | 490 | 490 | 480 | 480 | 489 | 476 | 478 | 490 | 488 | 488 | 496 | 486 | 486 | 491 |
| $\Phi_F$ (%) | 39.9 | 39.2 | 5.1 | 10.5 | 22.4 | 6.8 | 3.7 | 19.3 | 9.4 | 6.1 | 30.6 | 7.1 | 9.9 | 32.1 |

[a] Values determined in a 95/5 $H_2O$–THF (v/v) mixture.

 

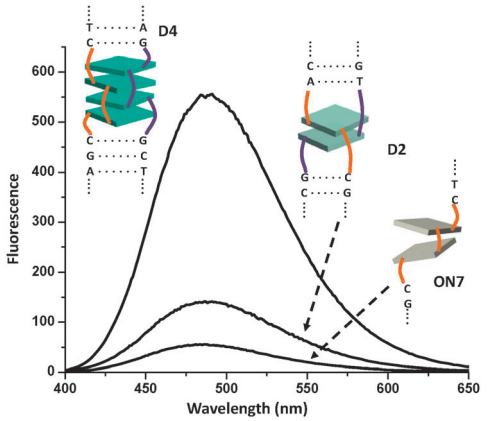


**Fig. 4** Fluorescence spectra of single strand **ON7** and hybrids **D2** and **D4**; conditions as in Fig 2.

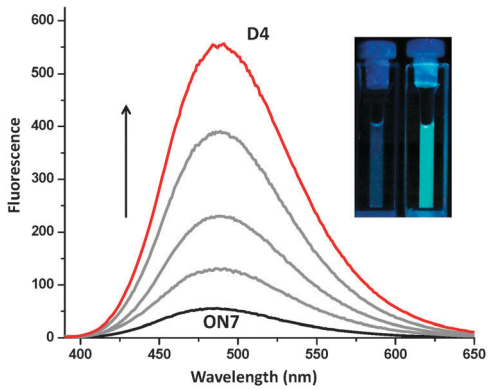


**Fig. 5** Titration of **ON7** (starting conc. 1.0 μM) by addition of **ON8** (individual steps = 0.25 μM); arrow indicates increasing **ON8** conc.; photo: AIE of **D4** (right) compared to single strand **ON7**; conditions as in Fig. 2.

($\Phi_F \sim 0.40$). These findings reflect a steady growth of the emission with an increasing degree of molecular aggregation, *i.e.* the compact arrangement of DATPEs effectively suppresses the intramolecular rotation.[42] The effect of AIE is best illustrated in the example shown in Fig. 5, which represents the change in fluorescence between single strand **ON7** and duplex **D4**. Duplex formation results in a 10-fold increased emission.

In conclusion, we have demonstrated that AIE can be controlled by DNA hybridization. Two AIE-active, DATPE building blocks were incorporated into oligonucleotides. Hybridization of complementary strands leads to molecular aggregation of the DATPE units. Quantum yields in hybrids reach values close to those of the monomers in the aggregated state. Considering the ease of their synthesis and their unique fluorescence properties, DATPEs are promising candidates for diagnostic probes or DNA-based nanostructures with special optical properties.

This work was supported by the Swiss National Foundation (Grant 200020-132581).

## Notes and references

1 N. C. Seeman, *Nature*, 2003, **421**, 427–431.
2 J. Wengel, *Org. Biomol. Chem.*, 2004, **2**, 277–280.
3 K. V. Gothelf and T. H. Labean, *Org. Biomol. Chem.*, 2005, **3**, 4023–4037.
4 N. L. Rosi and C. A. Mirkin, *Chem. Rev.*, 2005, **105**, 1547–1562.
5 J. M. Kinsella and A. Ivanisevic, *Langmuir*, 2007, **23**, 3886–3890.
6 F. A. Aldaye, A. L. Palmer and H. F. Sleiman, *Science*, 2008, **321**, 1795–1799.
7 M. Endo and H. Sugiyama, *ChemBioChem*, 2009, **10**, 2420–2443.
8 B. Sacca and C. M. Niemeyer, *Angew. Chem., Int. Ed.*, 2012, **51**, 58–66.
9 F. Diezmann and O. Seitz, *Chem. Soc. Rev.*, 2011, **40**, 5789–5801.
10 Y. N. Teo and E. T. Kool, *Chem. Rev.*, 2012, **112**, 4221–4245.
11 M. Kwak and A. Herrmann, *Chem. Soc. Rev.*, 2011, **40**, 5745–5755.
12 A. Heckel and M. Famulok, *Biochimie*, 2008, **90**, 1096–1107.
13 M. Meng, C. Ahlborn, M. Bauer, O. Plietzsch, S. A. Soomro, A. Singh, T. Müller, W. Wenzel, S. Brase and C. Richert, *ChemBioChem*, 2009, **10**, 1335–1339.
14 S. H. Weisbrod and A. Marx, *Chem. Commun.*, 2008, 5675–5685.
15 R. Varghese and H. A. Wagenknecht, *Chem. Commun.*, 2009, 2615–2624.
16 V. V. Filichev and E. B. Pedersen, in *Wiley Encycl. Chem. Biol.*, ed. T. P. Begley, Wiley, Hoboken, 2009, 1, pp. 493–524.
17 H. Kashida, X. Liang and H. Asanuma, *Curr. Org. Chem.*, 2009, **13**, 1065–1084.
18 V. L. Malinovskii, D. Wenger and R. Häner, *Chem. Soc. Rev.*, 2010, **39**, 410–422.
19 F. Seela and S. A. Ingale, *J. Org. Chem.*, 2010, **75**, 284–295.
20 O. Khakshoor and E. T. Kool, *Chem. Commun.*, 2011, **47**, 7018–7024.
21 E. Stulz, *Chem.–Eur. J.*, 2012, **18**, 4456–4469.
22 E. Socher, A. Knoll and O. Seitz, *Org. Biomol. Chem.*, 2012, **10**, 7363–7371.
23 J. Krim, M. Taourirte, C. Gruenewald, I. Krstic and J. W. Engels, *Synthesis*, 2013, 396–405.
24 F. D. Lewis, Y. F. Zhang and R. L. Letsinger, *J. Am. Chem. Soc.*, 1997, **119**, 5451–5452.
25 E. V. Bichenkova, A. R. Sardarian, A. N. Wilton, P. Bonnet, R. A. Bryce and K. T. Douglas, *Org. Biomol. Chem.*, 2006, **4**, 367–378.
26 I. Trkulja and R. Häner, *Bioconjugate Chem.*, 2007, **18**, 289–292.
27 I. Trkulja and R. Häner, *J. Am. Chem. Soc.*, 2007, **129**, 7982–7989.
28 S. Uno, C. Dohno, H. Bittermann, V. L. Malinovskii, R. Häner and K. Nakatani, *Angew. Chem., Int. Ed.*, 2009, **48**, 7362–7365.
29 K. C. Hannah and B. A. Armitage, *Acc. Chem. Res.*, 2004, **37**, 845–853.
30 H. Kashida, H. Asanuma and M. Komiyama, *Angew. Chem., Int. Ed.*, 2004, **43**, 6522–6525.
31 L. I. Markova, V. L. Malinovskii, L. D. Patsenker and R. Häner, *Org. Biomol. Chem.*, 2012, **10**, 8944–8947.
32 M. A. Abdalla, J. Bayer, J. O. Radler and K. Müllen, *Angew. Chem., Int. Ed.*, 2004, **43**, 3967–3970.
33 M. Balaz, A. E. Holmes, M. Benedetti, P. C. Rodriguez, N. Berova, K. Nakanishi and G. Proni, *J. Am. Chem. Soc.*, 2005, **127**, 4172–4173.
34 F. D. Lewis, L. G. Zhang, X. Y. Liu, X. B. Zuo, D. M. Tiede, H. Long and G. C. Schatz, *J. Am. Chem. Soc.*, 2005, **127**, 14445–14453.
35 R. Häner, F. Samain and V. L. Malinovskii, *Chem.–Eur. J.*, 2009, **15**, 5701–5708.
36 D. Wenger, V. L. Malinovskii and R. Häner, *Chem. Commun.*, 2011, **47**, 3168–3170.
37 F. Garo and R. Häner, *Angew. Chem., Int. Ed.*, 2012, **51**, 916–919.
38 J. G. Woller, J. K. Hannestad and B. Albinsson, *J. Am. Chem. Soc.*, 2013, **135**, 2759–2768.
39 O. N. Sancho, W. R. Browne and G. Roelfes, *Chem.–Eur. J.*, 2013, **19**, 2457–2461.
40 Z. Zhao, J. W. Lam and B. Z. Tang, *J. Mater. Chem.*, 2012, **22**, 23726–23740.
41 N. B. Shustova, T. C. Ong, A. F. Cozzolino, V. K. Michaelis, R. G. Griffin and M. Dinca, *J. Am. Chem. Soc.*, 2012, **134**, 15061–15070.
42 Y. Hong, J. W. Lam and B. Z. Tang, *Chem. Soc. Rev.*, 2011, **40**, 5361–5388.
43 Y. Hong, H. Xiong, J. W. Y. Lam, M. Haeussler, J. Liu, Y. Yu, Y. Zhong, H. H. Sung, I. D. Williams, K. S. Wong and B. Z. Tang, *Chem.–Eur. J.*, 2010, **16**, 1232–1245.
44 H. Tong, Y. Hong, Y. Dong, M. Haeussler, Z. Li, J. W. Lam, Y. Dong, H. H. Sung, I. D. Williams and B. Z. Tang, *J. Phys. Chem. B*, 2007, **111**, 11817–11823.
45 M. Wang, D. Zhang, G. Zhang and D. Zhu, *Chem. Commun.*, 2008, 4469–4471.
46 C. W. T. Leung, Y. Hong, S. Chen, E. Zhao, J. W. Y. Lam and B. Z. Tang, *J. Am. Chem. Soc.*, 2013, **135**, 62–65.
47 Y. Yu, J. Liu, Z. Zhao, K. M. Ng, K. Q. Luo and B. Z. Tang, *Chem. Commun.*, 2012, **48**, 6360–6362.
48 J. Kypr, I. Kejnovska, D. Renciuk and M. Vorlickova, *Nucleic Acids Res.*, 2009, **37**, 1713–1725.
49 Judging from circular dichroism spectroscopy, the presence of 70% TFE does not significantly affect the B-form conformation of the present hybrids (ESI†).